

# **Log Interpretation Parameters Determined from Chemistry, Mineralogy and Nuclear Forward Modeling**

Michael M. Herron and Susan L. Herron

Schlumberger-Doll Research  
Old Quarry Road, Ridgefield, CT 06877-4108

## **ABSTRACT**

The determination of suitable parameters to properly interpret log data in terms of porosity, clay content and water saturation is often arduous. For example, classical estimates of clay volume frequently use the range of observed gamma ray values over a depth interval as a clay calibration. An improved procedure presented here integrates core mineralogy and chemistry as well as nuclear forward modeling. Accurate mineralogy ( $\pm 2$  wt %) from the Dual-Range Fourier Transform Infrared (FT-IR) spectroscopy procedure is used. The chemical element analysis includes not only the major compositional elements but also all trace and minor elements that can significantly influence log responses. The chemical and mineralogical data are then used with nuclear forward modeling to provide the log response of logging sondes such as gamma ray, matrix density, hydrogen index, photoelectric absorption cross section, and thermal and epithermal neutron responses. It is then usually straightforward to see simple relationships between available logging variables and desired parameters.

Data from two example wells show that total clay content is linearly correlated with aluminum (Al). This is particularly useful since simulated aluminum concentration logs can be obtained in both open- and cased-hole environments from induced gamma ray spectroscopy sondes. With classical gamma ray interpretation, several reservoir intervals would be overlooked due to moderately high gamma ray levels. These same intervals have low aluminum concentrations. Thermal neutron porosity is close to total porosity only in the cleanest intervals. A simple relationship is observed between aluminum and the modeled thermal neutron porosity response. The Al-corrected neutron porosity agrees well with core porosity. The thermal neutron capture cross section, sigma matrix, also correlates linearly with aluminum. Most important logging parameters are demonstrated to be simply related to clay content and thus to aluminum. This integration of chemistry, mineralogy and nuclear response data is an efficient way of providing necessary parameters for accurate log interpretation.

## **INTRODUCTION**

Oilfield logging sondes do not directly measure desired formation properties such as lithology, porosity, and hydrocarbon saturation. Instead, these properties must be estimated from the measured variables such as total gamma ray activity, electron density, thermal neutron count rates, and electrical resistivity. The estimation procedure is

sometimes rather arbitrary. For example, it is common to use the range of observed total gamma ray activity to scale measurements between 0 % and 100 % shale. This procedure assumes a minimum clay content value for formations with the lowest gamma ray reading. Bhuyan and Passey<sup>1</sup> refined this procedure to scale between 0 % and 60 % clay, thereby including the observation that many shales are composed of 60% clay minerals and 40% non-clay minerals. Additional log correction parameters such as the shale neutron response or shale matrix thermal neutron capture cross section (referred to as sigma) are then estimated from the gamma ray or gamma ray-derived shale log. This sort of procedure is often followed in absence of core data for refinement.

This paper presents a methodology for calculating many of the parameters needed for log evaluation from core data. It further shows that these parameters can usually be quantitatively evaluated on a level-by-level basis from geochemical log data.

## EXPERIMENTAL METHODS

Core plug samples were provided from a well in Europe and a gas well in Texas. These two wells represent vastly different geological depositional environments and diagenetic histories. Core samples were crushed and split with a micro splitter into mineralogy and chemistry fractions. Mineralogy concentrations were obtained from the dual-range FT-IR procedure<sup>2</sup>. Concentrations of Si, Al, Fe, Ca, Mg, K, Na, H<sub>2</sub>O<sup>+</sup>, P, S, Cr, Mn, Ti, B, Rb, Sr, Y, Zr, Nb, Ba, Gd, Th, U and Loss on Ignition were determined by x-ray fluorescence, induction coupled plasma mass spectrometry, coulometry, Leco and neutron induced prompt gamma ray analysis. Concentrations of unmeasured rare earth elements were estimated from the measured rare earth concentrations and the North American Shale Composite relative abundances<sup>3</sup>.

Total gamma ray response was calculated as the weighted sum of thorium, uranium and potassium concentrations<sup>4</sup>. A number of nuclear parameters were calculated from the chemical concentrations and the SNUPAR code<sup>5</sup> including the thermal and epithermal neutron porosities, the thermal neutron capture cross section (also referred to as sigma), and the photoelectric absorption cross section.

## RESULTS AND DISCUSSION

Regressions were performed between computed gamma ray and several of the modeled nuclear parameters for both the European well samples and the Texas well samples. Identical regressions were performed between aluminum concentrations and the modeled nuclear parameters since aluminosilicates (clays) are a primary factor in determining such parameters. These regression results are summarized in Table 1 and displayed in Figures 1-10.

### European Well Samples

The clay content of siliciclastic reservoirs is one of the most important parameters to estimate accurately, because clay directly affects porosity, water saturation and permeability calculations as well as gas identification and overall reservoir quality. One of the primary ways to estimate the clay content is to use the total gamma ray signal. Figure 1a shows the European well total gamma ray signal, computed from the thorium, uranium and potassium concentrations, compared with the total clay content ( $\pm 2$  wt %) determined by FT-IR analysis. It is immediately clear that there is a general correlation between gamma ray and clay content, as shown by the solid line. There is no indication of a curved relationship

between GR and clay as has been suggested in numerous papers. There is however, a significant amount of scatter. Samples with a gamma ray readings of about 25 API have clay concentrations ranging from less than 5 wt % to nearly 30 wt %. A least squares fit is shown as the solid line with a correlation coefficient of  $r=0.86$  and a standard error of 8.7 wt % clay. The Bhuyan and Passey method, where the sample with the maximum gamma ray reading is assigned as 60 wt % clay and the sample with the minimum reading is assigned as 0 wt % clay, is shown as the dashed line in Figure 1a. This procedure leads to a biased estimate of the clay concentration in the European well samples as the clay concentration is underestimated in all but three samples.

The second common way to estimate clay from conventional log data involves scaling the separation between the neutron and density porosity log readings, both calculated on a sandstone matrix, from 0% clay at zero separation to about 60 wt % clay at the maximum separation in shales<sup>1</sup>. Figure 1b shows that there is a linear correlation between neutron-density separation and total clay. The correlation coefficient is 0.95 with a standard error of 4.6 wt % clay. While it is commonly assumed that the neutron-density separation is zero at zero percent clay, there is a surprising 5 p.u. offset in the modeled responses. Thus, in the absence of gas and with core calibration, neutron-density separation provides a good estimate of clay.

Figure 2 compares the aluminum concentrations and clay concentrations for the European well samples and shows that a similar correlation exists here. The correlation coefficient is  $r=0.98$  and the standard error is only 2.6 wt %. This correlation follows the trend previously established for numerous wells around the world<sup>6</sup>. Clay estimated from either the previously published aluminum-clay relationship or the optimized relationship shown in Figure 2 would be significantly more accurate for the European well than either estimate based on gamma ray response or on neutron-density separation. Since clay minerals are the major aluminosilicates in most sedimentary formations, a strong correlation with aluminum concentrations is expected unless perturbed by abnormal concentrations of micas or feldspars<sup>6</sup>.

Figures 3a and 3b compare gamma ray and aluminum with the thermal neutron capture cross section of the rock matrix (sigma matrix). This parameter is needed for quantitative analysis of thermal decay time measurements which are commonly made as part of well monitoring. The pertinent equation is

$$\Sigma_{\text{meas}} = \emptyset S_w \Sigma_w + \emptyset (1 - S_w) \Sigma_{\text{hc}} + (1 - \emptyset) \Sigma_{\text{ma}} \quad 1$$

where  $\Sigma_{\text{meas}}$  is the measured value,  $\emptyset$  is the porosity,  $S_w$  is the water saturation, and  $\Sigma_w$ ,  $\Sigma_{\text{hc}}$ , and  $\Sigma_{\text{ma}}$  refer to the capture cross sections of the water, hydrocarbon and rock matrix, respectively. The values for water and hydrocarbon are usually known for a locality. The matrix value is usually scaled according to gamma ray from a low value (often the quartz value of 4.7 capture units<sup>7</sup>) to a high value in shales. Figure 3a shows that sigma matrix for the European well samples correlates with gamma ray with a correlation coefficient of 0.89 and a standard error of 2.7 capture units. Correlation with aluminum is somewhat better (Fig. 3b) with a correlation coefficient of 0.94 and a standard error of 1.8 capture units. Clay is the major mineralogy component governing matrix sigma, so aluminum also correlates better with matrix sigma.

The primary variable affecting thermal neutron response is porosity. However, clay content is a close second due to the hydrogen atoms in the clay hydroxyl groups and, to a lesser degree, to other thermal neutron absorbers that also affect matrix sigma. The

pertinent equation governing interpretation of thermal neutron porosity can be approximated as

$$NPHI_{meas} = \phi S_w NPHI_w + \phi(1-S_w)NPHI_{hc} + (1-\phi)NPHI_{ma} \quad 2$$

where  $NPHI_{meas}$  is the measured neutron porosity and  $NPHI_w$ ,  $NPHI_{hc}$  and  $NPHI_{ma}$  refer to the thermal neutron response to water, hydrocarbon and the rock matrix, respectively. The values of  $NPHI_w$  and  $NPHI_{hc}$  are frequently similar due to similar hydrogen densities unless gas is present, so the value of  $NPHI_{ma}$  is often the largest uncertainty in evaluating equation 2. Figures 4a and 4b show that the gamma ray vs.  $NPHI_{ma}$  relationship exhibits much more scatter than the aluminum vs.  $NPHI_{ma}$  relationship. Note the similarities between the GR-clay (Fig. 1a) and GR- $NPHI_{ma}$  (Fig. 4a) patterns which demonstrate that clay content is the driving force in establishing  $NPHI_{ma}$ .

A similar pattern exists for the European well hydrogen index data. Figures 5a and 5b compare hydrogen index with gamma ray and with aluminum concentrations. As with Figures 1a and 1b, the correlation with aluminum is substantially better than with gamma ray. The linear correlation coefficient for HI:GR is 0.76; the correlation coefficient for HI:Al is 0.97. Again, this reflects the more reliable relationship between clay and Al concentrations. The equation governing hydrogen index interpretation is analogous to that for NPHI.

#### Texas Well Samples

The Texas gas well samples are an interesting contrast to the European well samples because oilfield operators in the area are aware of the untrustworthiness of gamma ray for estimating clay or other parameters due to the sporadic presence of radioactive volcanic ash layers. These ash layers were not sampled in the core study and, interestingly, in the layers that were sampled, gamma ray correlates strongly with clay and modeled nuclear and petrophysical parameters.

Figure 6a shows that gamma ray correlates strongly with total clay content with a correlation coefficient of 0.98. However, since the lowest gamma ray samples contain about 20 wt % clay, a simple scaling of gamma ray from 0 to 60 wt % clay produces errors of 20 wt % in the reservoir samples. The separation between neutron and density porosities, both computed on a sandstone matrix, also linearly varies with total clay content ( $r=0.99$ ), but again there is a significant offset at zero clay (Fig. 6b). Figure 7 shows that aluminum correlates strongly with total clay ( $r=0.98$ ) but there is significant aluminum at zero clay due to the sizable feldspar content. Each of these variables correlates well with total clay, but the gamma ray is known to be sporadically unreliable in the area, and these samples come from a gas well where the neutron-density separation fails, so the most reliable clay estimate would come from the aluminum. The default clay-aluminum relationship for feldspar-rich sands<sup>6</sup> works nearly as well as the regression on these samples.

Figures 8-10 show that, for the core samples analyzed, both gamma ray or aluminum correlate well with sigma matrix, neutron porosity matrix, hydrogen index and cation exchange capacity. The regression parameters are given in Table 1. Use of either gamma ray or aluminum with the regression parameters given in Table 1 would give acceptable estimates of the petrophysical parameters provided no volcanic ash were encountered. Again, the separation between neutron and density is inapplicable due to the occurrence of low density, low hydrogen content gas.

### Log Example

How does the use of core calibration improve the estimation of clay content? Figure 11 shows clay content determined from the aluminum log in the Texas well as a function of depth. For comparison, the total clay content in the 15 core samples is shown as filled circles. There is reasonable agreement, given the usual core-log comparison problems. Figure 11 also shows the clay content estimated from the gamma ray without the core calibration and using the scaling of Bhuyan and Passey (1994). This estimate is slightly high, relative to the aluminum estimate, in the shales. More importantly, it misses sands at 3600-3700 ft and 4950 ft. These sands are believed to be excessively radioactive due to volcanic material. Note that the gamma ray-based clay estimate performs reasonably well over the cored interval.

Figure 12 shows that using the core calibrated regression results from Table 1 gives a gamma ray-based clay estimate that is in better agreement with the aluminum-based estimate. It still misses the sands with volcanic material but over much of the profile there is little difference between the two estimates.

## **SUMMARY AND CONCLUSIONS**

A methodology is presented for calculating many of the parameters needed for formation evaluation of log data. First, a core data set is established consisting of accurate mineralogy and a specific set of chemical elemental concentrations. Second, these basic data are used in nuclear forward modeling to determine a variety of matrix properties such as matrix thermal neutron capture cross section, matrix thermal neutron porosity, and matrix hydrogen index. Other computed properties include total clay and total gamma ray response.

Finally, regression equations are constructed where desired petrophysical parameters are set as a function of measurable parameters such as gamma ray or aluminum. We find that in sand and shaly sandstone environments, clay minerals are the dominant source of parameter variance. Since clays are the major aluminosilicates in such environments, it is also observed that the petrophysical parameters usually show simple correlations with aluminum concentrations. Fortunately, such an aluminum log can be obtained in both open- and cased-hole environments<sup>6</sup>.

## REFERENCES

1. Bhuyan, K. and Passey, Q.R.: "Clay estimation from GR and Neutron-Density porosity logs", paper DDD, Transactions 35th Annual SPWLA Logging Symposium, 1994, p. DDD1-15.
2. Herron, M.M., Matteson, A., and Gustavson, G.: "Dual-range FT-IR mineralogy and the analysis of sedimentary formations", this proceedings.
3. McLennan, S.M., Nance, W.B. and Taylor, S.R.: "The North American Shale Composite," *Geochemica et Cosmochimica Acta*, .
4. Ellis, D.V.: "Well logging for earth scientists", Elsevier, New York, 532 p.
5. McKeon, D.C. and Scott, H.D.: "SNUPAR - A nuclear parameter code for nuclear geophysics applications", *Nuclear Geophysics* (1988), v. 2, 215-230.
6. Herron, S.L. and Herron, M.M.: "Quantitative lithology: an application for open and cased hole spectroscopy", Transactions of the SPWLA 37th Annual Logging Symposium, New Orleans, LA, June 16-19, 1996, Paper E.
7. Herron, M.M. and Matteson, A.: "Elemental composition and nuclear parameters of some common sedimentary minerals", *Nuclear Geophysics* (1993), v. 7, 383-406.

Table 1. Linear regression parameters for the European and Texas wells.

Variable	Slope	Parameter	Offset	r	Std. Error
<i>European Well Core Samples</i>					
Clay	0.50	GR	-2.7	0.86	8.7 % clay
	1.84	N-D	-5.9	0.95	4.6
	5.88	Al	-2.3	0.98	2.6
Sigma	0.175	GR	6.7	0.89	2.7 c.u.
	1.91	Al	7.7	0.94	1.8
NPHI	0.20	GR	2.6	0.81	4.3 p.u.
	2.44	Al	2.1	0.98	1.2
HI	0.0012	GR	0.0062	0.76	0.03
	0.15	Al	-0.0017	0.97	0.01
<i>Texas Well Core Samples</i>					
Clay	0.57	GR	-7.6	0.98	1.9 % clay
	2.94	N-D	-13.8	0.99	1.1
	13.1	Al	-51.9	0.98	1.6
Sigma	0.175	GR	7.8	0.98	0.5 c.u.
	3.98	Al	-5.5	0.97	0.5
NPHI	0.14	GR	3.2	0.96	0.2 p.u.
	3.16	Al	-7.5	0.96	0.5
HI	0.0008	GR	0.003	0.95	0.003
	0.018	Al	-0.06	0.96	0.003

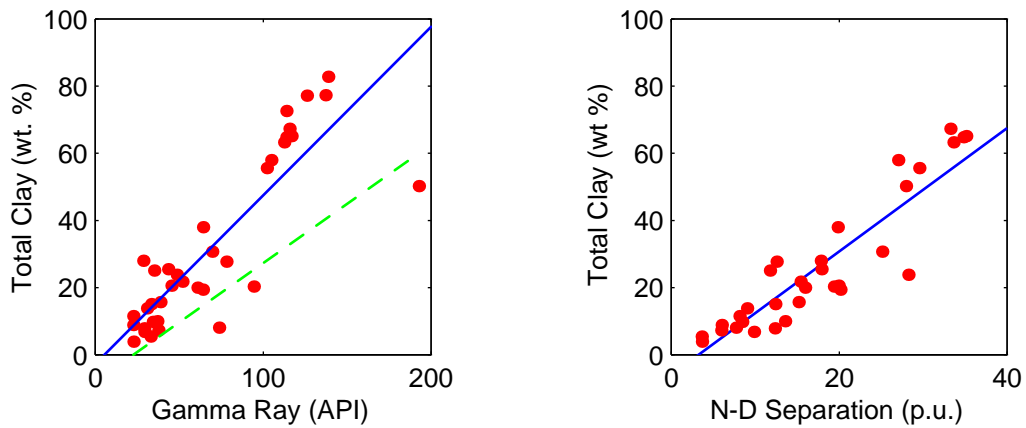


Figure 1. a) Total clay concentration compared to computed gamma ray response (a) for the European core data. The solid line is the least squares fit; the dashed line follows the logic of Bhuyan and Passey (1994). b) Total clay content compared to the separation between neutron porosity and density porosity (both on a sandstone matrix) is a slightly better fit but shows a surprising offset of about 5 p.u. at 0 % clay.

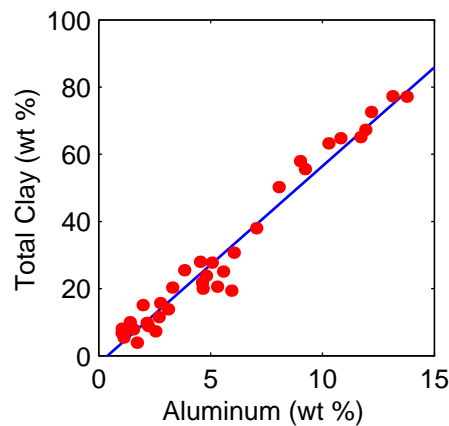


Figure 2. Relationship between aluminum and total clay shows a very tight linear relationship.

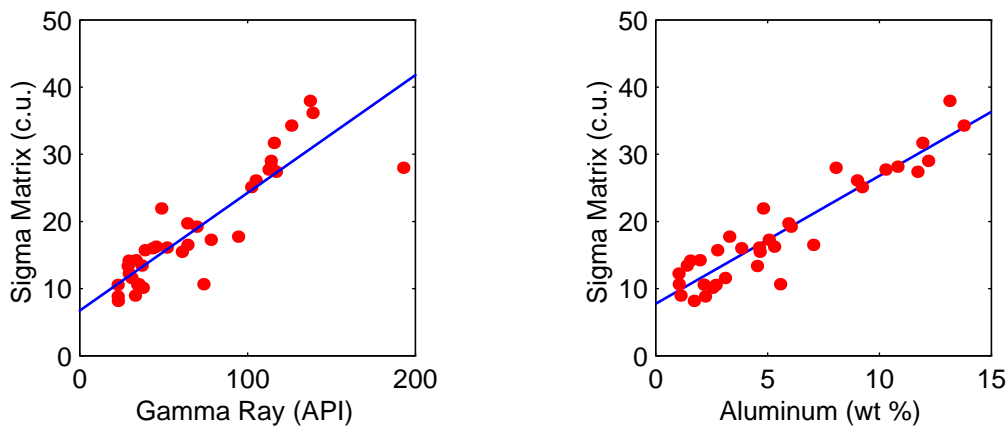


Figure 3. a) Sigma matrix compared to total gamma ray for the European well samples. b) Sigma matrix compared to aluminum for the same samples.



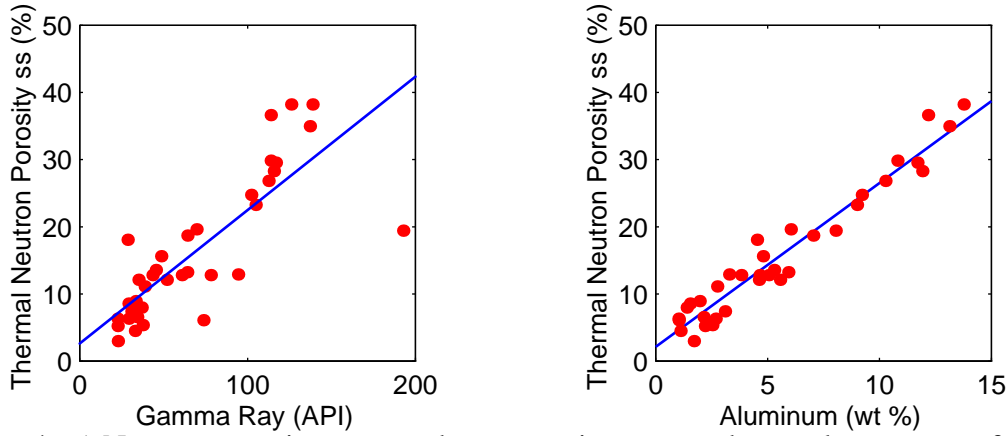


Figure 4. a) Neutron porosity on a sandstone matrix compared to total gamma ray for the European well samples. b) neutron porosity compared to aluminum for the same samples.

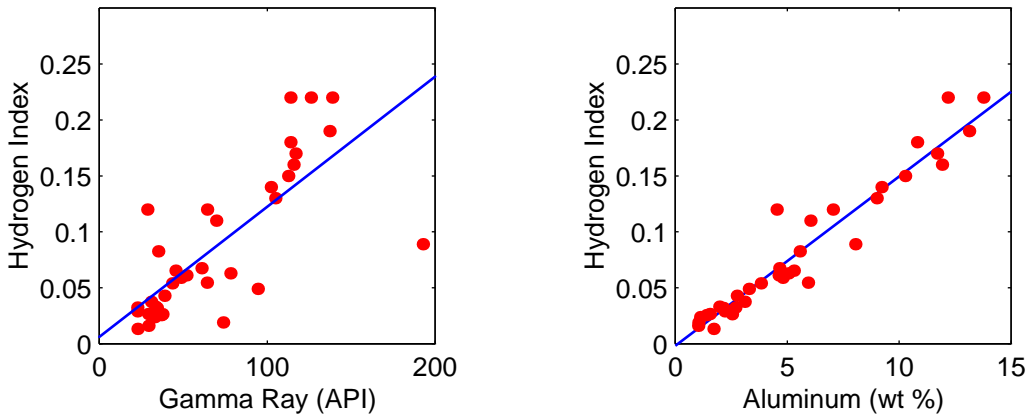


Figure 5. a) Hydrogen index matrix compared to total gamma ray for the European well samples. b) hydrogen index matrix compared to aluminum for the same samples.

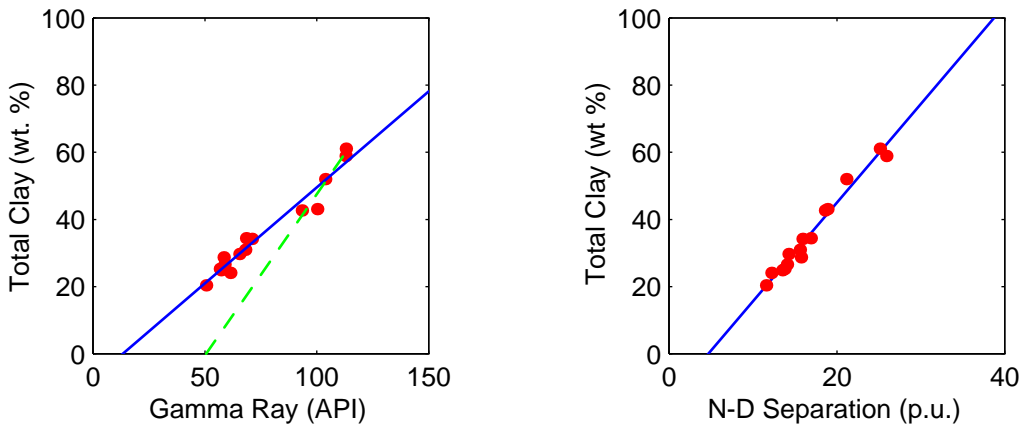


Figure 6. a) Total clay concentration compared to computed gamma ray response (a) for the Texas core data. The solid line is the least squares fit; the dashed line follows the logic of Bhuyan and Passey (1994). b) Total clay content compared to the separation between neutron porosity and density porosity (both on a sandstone matrix) again shows a surprising offset of about 5 p.u. at 0 % clay.

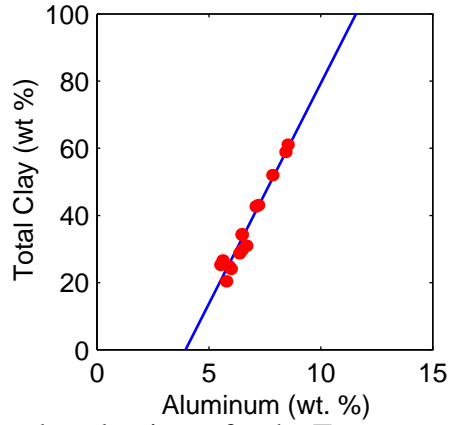


Figure 7. Total clay compared to aluminum for the Texas samples. The solid line is the least squares regression result.

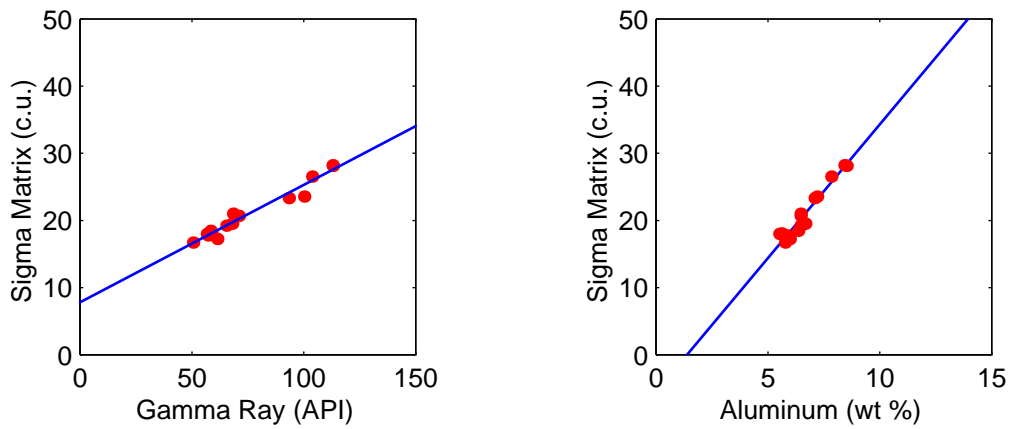


Figure 8. a) Sigma matrix compared to total gamma ray for the Texas well samples. b) Sigma matrix compared to aluminum for the same samples.

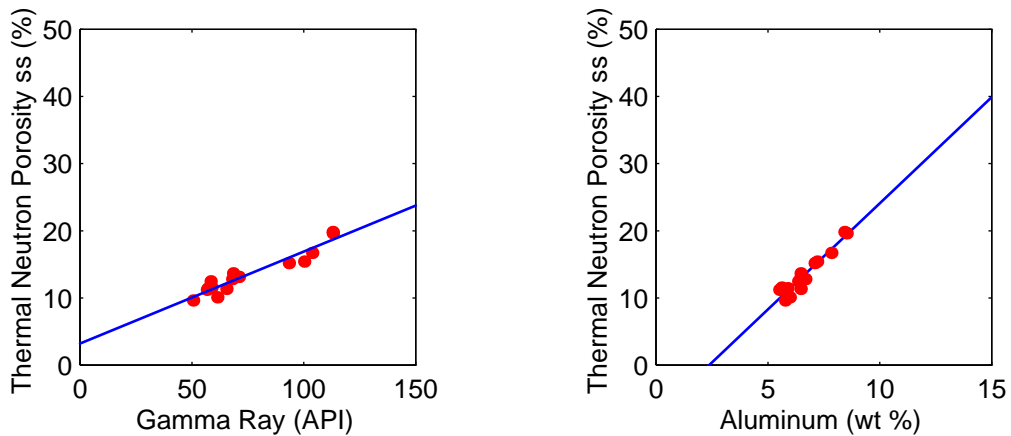


Figure 9. a) Matrix thermal neutron response on a sandstone matrix compared to total gamma ray for the European well samples. b) Matrix thermal neutron response compared to aluminum for the same samples.

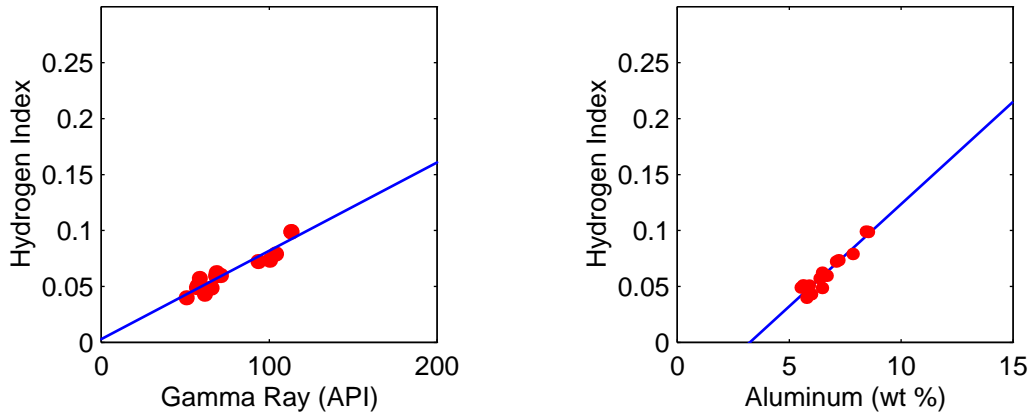


Figure 10. a) Hydrogen index compared to total gamma ray for the Texas well samples. b) Hydrogen index compared to aluminum for the same samples.

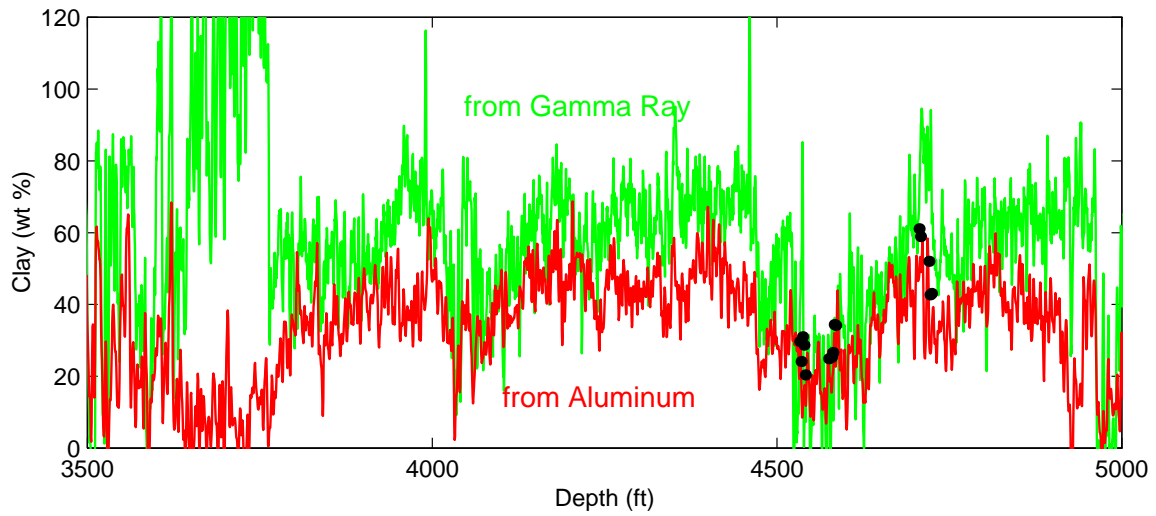


Figure 11. Clay estimation from gamma ray and the Bhuyan and Passey (1994) methodology overestimates clays in the shales and completely misses sands at 3600-3700 ft and 4950 ft but does well in the reservoir at 4550 ft.

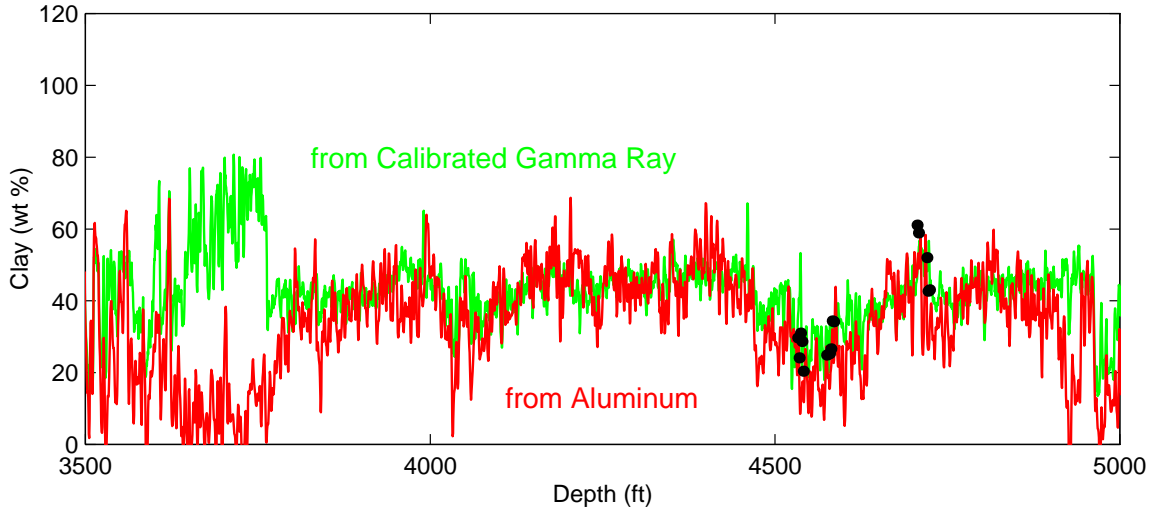


Figure 12. Clay estimation from the core-calibrated gamma ray still misses sands at 3600-3700 ft and 4950 ft but does well in the reservoir at 4550 ft.